



LMI-BASED H_∞ CONTROL OF A FULL-SCALE BUILDING WITH ACTIVE BRACING SYSTEM

Jong-Cheng WU¹, Hsin-Hsien CHIH²

SUMMARY

Recently, more and more experimental studies indicate that a mature active control design toward practical implementation requires the consideration of robustness requirements in the design process, which includes the performance robustness on reducing the tracking error and in resistance to the external disturbance and measurement noise, and the stability robustness with respect to system uncertainty. The H_∞ control method, among all advanced control strategies, provides a fine approach to take these robustness requirements into account for the robust controller design. In this paper, an efficient solution procedure of H_∞ dynamic output feedback controller for the control of civil structures based on solving a set of linear matrix inequalities (LMI), the so-called LMI-based robust H_∞ control, is introduced. For verifying its applicability, extensive numerical simulations under the excitations of the 1940 NS El Centro and 1995 Kobe earthquakes were conducted on a full-scale three-story seismic-excited building model equipped with an active bracing system. In the simulation, the system uncertainty is assumed in the controller design and the employment of acceleration feedback is emphasized for practical consideration. Through the LMI-based solution procedure, the efficiency of H_∞ controller design is approved. From the simulation results, it is demonstrated that the performance of the H_∞ controllers presented is remarkable and robust, and therefore it is suitable for application to civil engineering buildings for aseismic protection.

INTRODUCTION

Over the past two decades, the use of active control on civil engineering structures for the suppression of seismic-induced and wind-induced vibrations has attracted a great deal of attention because of its remarkable effectiveness [e.g., Soong (1990), Kobori et al (1998), Casciati (2002)]. Considerable research efforts on the experimental verification using shake table tests and wind tunnel tests have been made and presented in the literatures [e.g., Chung *et al.* (1989), Dyke *et al.* (1994a,b), Wu (2000), etc., Wu *et al.* (2002), Wu *et al.* (2003)]. The valuable experience gained through these tests indicate that a mature active control design toward practical implementation requires the consideration of

¹ Associate Professor, Department of Civil Engineering, Tamkang University, Taipei, Taiwan.

² Former Graduate Student, Department of Civil Engineering, Tamkang University, Taipei, Taiwan.

robustness requirements in the design process, that is, the performance robustness in reducing the tracking error and in resistance to the external disturbance and measurement noise, and the stability robustness with respect to the existence of system uncertainty [Zhou and Doyle (1998)]. In particular, the stability robustness to uncertainty is relatively important because the properties of most civil structures are not easy to predict perfectly. Among the advanced control strategies proposed in many literatures [e.g. Kobori (1998), Casciati (2002)], H^∞ control strategy is particularly useful in designing the robust controller because these robustness requirements in a way can be interpreted as the H^∞ norm of transfer function to be smaller than a given value.

The solution computation of the H^∞ controller has been broadly discussed in the control community in the past decades [Basar and Bernhard (1991)]. Among all, two typical literatures, i.e., [Glover *et al.* (1988)] and [Doyle *et al.* (1989)], presented a numerically efficient solution methodology by using two algebraic Riccati equations. However, its application is restricted to the so-called regular control system (i.e., \mathbf{D}_{12} and \mathbf{D}_{21} in Eqs. (4) and (5) have full column ranks). Later, a new solution methodology based on the solution of linear matrix inequalities (LMI), directly derived from the Bounded Real Lemma, is proposed by [Gahinet, P. and Apkarian, P (1994)], referred to as the LMI-based H^∞ control. The theorem of the LMI-based solution method is more straightforward and no restriction is required. Besides, its solution procedure is efficient in computation. According to these advantages, in this paper, the H^∞ controllers that take the robustness requirements into account based on the LMI approach are designed to control a full-scale seismic-excited building for verifying its applicability toward implementation on civil engineering structures. The full-scale building considered herein is made of a three-story spatial steel rigid frame and equipped with an active bracing system on the first floor (see Fig. 8 in simulation section). It was once constructed on the shake table of the National Center for Research on Earthquake Engineering (NCREE) in Taiwan for the verification of active control. The numerical model of the building was constructed and presented in [Wu (2000)] and its validity has been well verified through shake table tests. Therefore, it can be esteemed to be suitably used for numerical simulation if other control methods are to be employed. Extensive numerical simulations based on this numerical model were conducted in this investigation to verify the control applicability and the comparisons with those using LQG (Linear Quadratic Gaussian) control are also made for the demonstration of control performance.

FORMULATION

In this section, we will firstly describe the basic concept of generalized H^∞ control for a controlled system, followed by a brief description of the LMI-based procedures for solving the H^∞ controller proposed by [Gahinet, P. and Apkarian, P (1994)]. Secondly, for controlling a physical seismic-excited structure, the concept of robust control with the robustness requirements specified is further introduced, and thirdly the derivation of forming a H^∞ control problem via these robustness requirements is described so that the LMI-based procedures can be utilized in consequence.

Generalized H^∞ Control

A typical block diagram of generalized H^∞ controlled system is shown in Fig.1. The generalized plant system is denoted by $\mathbf{G}(s)$, which has two sets of inputs \mathbf{W} and \mathbf{U} , and two sets of outputs \mathbf{z} and \mathbf{y} . In Fig. 1, the m_1 -dimensional vector \mathbf{W} is the exogenous input, which might involve the external disturbance, measurement noise or reference signal, while the m_2 -dimensional vector \mathbf{U} is the control command from the controller. The p_1 -dimensional vector \mathbf{z} contains the physical quantities to be attenuated, referred to as the controlled output, while the p_2 -dimensional vector \mathbf{y} contains the measurements to be used as the feedback quantities, referred to as the measured output. The block expressed by $\mathbf{K}(s)$ represents the transfer function of a dynamic output feedback controller to be designed. In the concept of H^∞ control, the objective is to design an appropriate dynamic output feedback controller $\mathbf{K}(s)$ such that the transfer

function from \mathbf{W} to \mathbf{z} , denoted as $\mathbf{H}_{z\mathbf{W}}$, is stable and its H^∞ norm, denoted as $\|\mathbf{H}_{z\mathbf{W}}\|_\infty$, is smaller than a given attenuation value γ , i.e., $\|\mathbf{H}_{z\mathbf{W}}\|_\infty < \gamma$. The H^∞ norm of the transfer function x_3 is defined by

$$\|\mathbf{H}_{z\mathbf{W}}\|_\infty = \text{Sup}_{\mathbf{W}(t) \in R} \frac{\|\mathbf{z}(t)\|_2}{\|\mathbf{W}(t)\|_2} \quad (1)$$

where $\|\cdot\|_2 = \left(\int_0^\infty (\cdot)^T (\cdot) dt \right)^{1/2}$ is the L_2 norm of a time-variant vector. In other words, the H^∞ norm is the worst case of the ratio of the output L_2 norm versus the input L_2 norm. It can be easily shown that the H^∞ norm in Eq. (1) can be further rewritten as

$$\|\mathbf{H}_{z\mathbf{W}}\|_\infty = \text{Sup}_{\omega \in R} \bar{\sigma}(\mathbf{H}_{z\mathbf{W}}(j\omega)) \quad (2)$$

in which $j = \sqrt{-1}$ and $\bar{\sigma}(\cdot)$ denotes the maximum singular value. Therefore, the condition $\|\mathbf{H}_{z\mathbf{W}}\|_\infty < \gamma$ obviously implies $\|\mathbf{z}(t)\|_2 < \gamma \|\mathbf{W}(t)\|_2$.

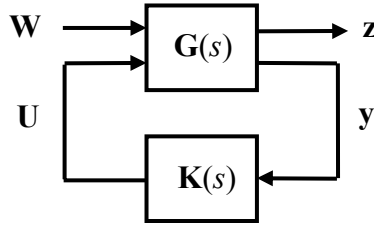


Fig.1: Block Diagram of a Generalized H^∞ Control

In the state space, the generalized plant $\mathbf{G}(s)$ can be represented by the state equation expressed by

$$\dot{\mathbf{X}} = \mathbf{A}\mathbf{X} + \mathbf{B}_1\mathbf{W} + \mathbf{B}_2\mathbf{U} \quad (3)$$

$$\mathbf{z} = \mathbf{C}_1\mathbf{X} + \mathbf{D}_{11}\mathbf{W} + \mathbf{D}_{12}\mathbf{U} \quad (4)$$

$$\mathbf{y} = \mathbf{C}_2\mathbf{X} + \mathbf{D}_{21}\mathbf{W} + \mathbf{D}_{22}\mathbf{U} \quad (5)$$

in which $\mathbf{A} \in R^{n \times n}$, $\mathbf{B}_1 \in R^{n \times m_1}$, $\mathbf{B}_2 \in R^{n \times m_2}$, $\mathbf{C}_1 \in R^{p_1 \times n}$, $\mathbf{D}_{11} \in R^{p_1 \times m_1}$, $\mathbf{D}_{12} \in R^{p_1 \times m_2}$, $\mathbf{C}_2 \in R^{p_2 \times n}$, $\mathbf{D}_{21} \in R^{p_2 \times m_1}$, $\mathbf{D}_{22} \in R^{p_2 \times m_2}$; $(\mathbf{A}, \mathbf{B}_2)$ is stabilizable and $(\mathbf{A}, \mathbf{C}_2)$ is detectable. Likely, the state equation of the controller $\mathbf{K}(s)$ can be expressed by

$$\dot{\mathbf{X}}_k = \mathbf{A}_k\mathbf{X}_k + \mathbf{B}_k\mathbf{y} \quad (6)$$

$$\mathbf{U} = \mathbf{C}_k\mathbf{X}_k + \mathbf{D}_k\mathbf{y} \quad (7)$$

in which $\mathbf{A}_k \in R^{k \times k}$, $\mathbf{B}_k \in R^{k \times p_2}$, $\mathbf{C}_k \in R^{m_2 \times k}$, $\mathbf{D}_k \in R^{m_2 \times p_2}$ are constant matrices to be determined by the control theory. For simplifying the following derivation, another measured output $\bar{\mathbf{y}} = \mathbf{y} - \mathbf{D}_{22}\mathbf{U} = \mathbf{C}_2\mathbf{X} + \mathbf{D}_{21}\mathbf{W}$ instead of \mathbf{y} is firstly used in Eqs. (6) and (7). This assumption will be eliminated later by a simple transformation described in the subsequent section. Thus, the corresponding matrices of the controller in Eqs. (6) and (7) are denoted by $\bar{\mathbf{A}}_k$, $\bar{\mathbf{B}}_k$, $\bar{\mathbf{C}}_k$, $\bar{\mathbf{D}}_k$, respectively. Hence, the closed-loop transfer function $\mathbf{H}_{z\mathbf{W}}$ can be obtained by substituting Eq. (7) into Eq. (4) as

$$\mathbf{H}_{z\mathbf{W}}(s) = \mathbf{D}_{cl} + \mathbf{C}_{cl}(s\mathbf{I} - \mathbf{A}_{cl})^{-1}\mathbf{B}_{cl} \quad (8)$$

$$\mathbf{A}_{cl} = \mathbf{A}_0 + \beta \boldsymbol{\theta} \boldsymbol{\zeta} ; \quad \mathbf{B}_{cl} = \mathbf{B}_0 + \beta \boldsymbol{\theta} \boldsymbol{\zeta}_{21} ; \quad (9)$$

$$\mathbf{C}_{cl} = \mathbf{C}_0 + \boldsymbol{\zeta}_{12} \boldsymbol{\theta} \boldsymbol{\zeta} ; \quad \mathbf{D}_{cl} = \mathbf{D}_{11} + \boldsymbol{\zeta}_{12} \boldsymbol{\theta} \boldsymbol{\zeta}_{21}$$

in which

$$\begin{aligned} \mathbf{A}_0 &= \begin{bmatrix} \mathbf{A} & 0 \\ 0 & 0_k \end{bmatrix}; \mathbf{B}_0 = \begin{bmatrix} \mathbf{B}_1 \\ 0 \end{bmatrix}; \mathbf{C}_0 = [\mathbf{C}_1 \quad 0]; \boldsymbol{\beta} = \begin{bmatrix} 0 & \mathbf{B}_2 \\ \mathbf{I}_k & 0 \end{bmatrix}; \boldsymbol{\varsigma} = \begin{bmatrix} 0 & \mathbf{I}_k \\ \mathbf{C}_2 & 0 \end{bmatrix}; \\ \zeta_{12} &= [0 \quad \mathbf{D}_{12}]; \zeta_{21} = \begin{bmatrix} 0 \\ \mathbf{D}_{21} \end{bmatrix}; \boldsymbol{\theta} = \begin{bmatrix} \bar{\mathbf{A}}_k & \bar{\mathbf{B}}_k \\ \bar{\mathbf{C}}_k & \bar{\mathbf{D}}_k \end{bmatrix} \end{aligned} \quad (10)$$

In Eq. (10), 0_k represents the $(k \times k)$ -dimensional matrix with 0 entries, \mathbf{I}_k represents the $(k \times k)$ -dimensional identity matrix.

LMI-based Procedure

According to the Bounded Real Lemma [e.g., Gahinet and Apkarian (1994), Zhou and Doyle (1998)], the controller $\mathbf{K}(s)$ in Fig. 1 exists such that $\|\mathbf{H}_{zW}\|_\infty < \gamma$ if and only if there exists a symmetric matrix $\mathbf{X}_{cl} \in R^{(n+k) \times (n+k)} > 0$ (i.e., \mathbf{X}_{cl} positive definite) such that

$$\begin{bmatrix} \mathbf{A}_{cl}^T \mathbf{X}_{cl} + \mathbf{X}_{cl} \mathbf{A}_{cl} & \mathbf{X}_{cl} \mathbf{B}_{cl} & \mathbf{C}_{cl}^T \\ \mathbf{B}_{cl}^T \mathbf{X}_{cl} & -\gamma \mathbf{I} & \mathbf{D}_{cl}^T \\ \mathbf{C}_{cl} & \mathbf{D}_{cl} & -\gamma \mathbf{I} \end{bmatrix} < 0 \quad (11)$$

In other words, the controller matrices $(\bar{\mathbf{A}}_k, \bar{\mathbf{B}}_k, \bar{\mathbf{C}}_k, \bar{\mathbf{D}}_k)$ and a positive definite \mathbf{X}_{cl} can be found to satisfy Eq. (11) if and only if $\|\mathbf{H}_{zW}\|_\infty < \gamma$. The equation (11) can be further rewritten as

$$\boldsymbol{\Psi}_{\mathbf{X}_{cl}} + \boldsymbol{\psi}^T \boldsymbol{\theta}^T \boldsymbol{\xi}_{\mathbf{X}_{cl}} + \boldsymbol{\zeta}_{\mathbf{X}_{cl}}^T \boldsymbol{\theta} \boldsymbol{\psi} < \mathbf{0} \quad (12)$$

in which

$$\boldsymbol{\Psi}_{\mathbf{X}_{cl}} = \begin{bmatrix} \mathbf{A}_0^T \mathbf{X}_{cl} + \mathbf{X}_{cl} \mathbf{A}_0^T & \mathbf{X}_{cl} \mathbf{B}_0 & \mathbf{C}_0^T \\ \mathbf{B}_0^T \mathbf{X}_{cl} & -\gamma \mathbf{I} & \mathbf{D}_{11}^T \\ \mathbf{C}_0 & \mathbf{D}_{11} & -\gamma \mathbf{I} \end{bmatrix} \quad (13)$$

$$\boldsymbol{\psi} = [\boldsymbol{\varsigma}, \zeta_{21}, 0_{(k+p_2) \times p_1}]; \boldsymbol{\xi}_{\mathbf{X}_{cl}} = [\boldsymbol{\beta}^T \mathbf{X}_{cl}, 0_{(k+m_2) \times m_1}, \zeta_{12}^T]$$

Note that Eq. (13) is a linear matrix inequality (LMI) for either $\boldsymbol{\theta}$ or \mathbf{X}_{cl} individually, but not for both. By partitioning \mathbf{X}_{cl} and \mathbf{X}_{cl}^{-1} in the following manner

$$\mathbf{X}_{cl} = \begin{bmatrix} \mathbf{S} & \mathbf{N} \\ \mathbf{N}^T & * \end{bmatrix}; \mathbf{X}_{cl}^{-1} = \begin{bmatrix} \mathbf{R} & \mathbf{M} \\ \mathbf{M}^T & * \end{bmatrix} \quad (14)$$

in which $\mathbf{R}, \mathbf{S} \in R^{n \times n}$; $\mathbf{M}, \mathbf{N} \in R^{n \times k}$, and employing the projection lemma [Gahinet and Apkarian (1994)], several manipulations for Eq. (12) lead to two LMIs for \mathbf{R} and \mathbf{S} (the detail derivation is described in the **Appendix** for the reader interest), i. e.,

$$\begin{bmatrix} \mathbf{N}_R & 0 \\ 0 & \mathbf{I}_{m_1} \end{bmatrix}^T \begin{bmatrix} \mathbf{A}\mathbf{R} + \mathbf{R}\mathbf{A}^T & \mathbf{R}\mathbf{C}_1^T & \mathbf{B}_1 \\ \mathbf{C}_1\mathbf{R} & -\gamma \mathbf{I} & \mathbf{D}_{11} \\ \mathbf{B}_1^T & \mathbf{D}_{11}^T & -\gamma \mathbf{I} \end{bmatrix} \begin{bmatrix} \mathbf{N}_R & 0 \\ 0 & \mathbf{I}_{m_1} \end{bmatrix} < 0 \quad (15)$$

$$\begin{bmatrix} \mathbf{N}_S & 0 \\ 0 & \mathbf{I}_{p_1} \end{bmatrix}^T \begin{bmatrix} \mathbf{A}\mathbf{S} + \mathbf{A}^T\mathbf{S} & \mathbf{S}\mathbf{B}_1^T & \mathbf{C}_1^T \\ \mathbf{B}_1^T\mathbf{S} & -\gamma \mathbf{I} & \mathbf{D}_{11} \\ \mathbf{B}_1^T & \mathbf{D}_{11}^T & -\gamma \mathbf{I} \end{bmatrix} \begin{bmatrix} \mathbf{N}_R & 0 \\ 0 & \mathbf{I}_{p_1} \end{bmatrix} < 0 \quad (16)$$

in which \mathbf{N}_R and \mathbf{N}_S are the null base matrices of $(\mathbf{B}_2^T \quad \mathbf{D}_{21}^T)$ and $(\mathbf{C}_2 \quad \mathbf{D}_{21})$, respectively. In addition, the positive definiteness of \mathbf{X}_{cl} can lead to another LMI for \mathbf{R} and \mathbf{S} as

$$\begin{bmatrix} \mathbf{R} & \mathbf{I} \\ \mathbf{I} & \mathbf{S} \end{bmatrix} \geq 0 \quad (17)$$

[Packard et al. (1991)]. Hence, Eqs. (15)-(17) are the three basic LMIs in solving the H^∞ controller.

Above all, the LMI-based solution procedure for the H^∞ controller can be summarized in the following:

1. Use Matlab LMI Toolbox to solve γ , \mathbf{R} and \mathbf{S} by constructing a minimization problem with the objective function

$$J = \gamma + \alpha \cdot \text{Trace}(\mathbf{R}) + \beta \cdot \text{Trace}(\mathbf{S}) \quad (18)$$

subject to three LMI constraints described in Eqs. (15)-(17). In addition, one more constraint expressed by

$$\gamma > 0.5 \gamma_{\min} \quad (19)$$

can be also used to restrict the value of γ . In Eq. (18), α , β are two given weightings to modulate the trace of \mathbf{R} and \mathbf{S} , and the value of γ_{\min} in Eq. (19) is given to confine the lower bound of γ . Minimization of the trace of \mathbf{R} and \mathbf{S} is helpful in slowing down the dynamics of the controller for facilitating implementation.

2. From the identity

$$\mathbf{M}\mathbf{N}^T = \mathbf{I} - \mathbf{R}\mathbf{S} \quad (20)$$

, which is induced from Eq. (14), the matrices $\mathbf{M}, \mathbf{N} \in R^{n \times k}$ with full column rank can be obtained by using the singular value decomposition. Thus, by substituting \mathbf{M} and \mathbf{N} into an identity

$$\begin{bmatrix} \mathbf{S} & \mathbf{I} \\ \mathbf{N}^T & 0 \end{bmatrix} = \mathbf{X}_{\text{cl}} \begin{bmatrix} \mathbf{I} & \mathbf{R} \\ 0 & \mathbf{M}^T \end{bmatrix} \quad (21)$$

, which can be also deduced from Eq. (14), the matrix $\mathbf{X}_{\text{cl}} \in R^{(n+k) \times (n+k)}$ can be obtained.

3. Construct a minimization problem by Matlab LMI Toolbox to solve the controller matrices $\bar{\mathbf{A}}_k \in R^{k \times k}$, $\bar{\mathbf{B}}_k \in R^{k \times p_2}$, $\bar{\mathbf{C}}_k \in R^{m_2 \times k}$, $\bar{\mathbf{D}}_k \in R^{m_2 \times p_2}$ in θ with the objective function

$$J = \text{Trace}(\bar{\mathbf{A}}_k) \quad (22)$$

subject to the LMI constraint described in Eq. (12).

4. Once $\bar{\mathbf{A}}_k$, $\bar{\mathbf{B}}_k$, $\bar{\mathbf{C}}_k$, $\bar{\mathbf{D}}_k$ is obtained, the assumption of using measured output $\bar{\mathbf{y}} = \mathbf{y} - \mathbf{D}_{22}\mathbf{U} = \mathbf{C}_2\mathbf{X} + \mathbf{D}_{21}\mathbf{W}$ to replace \mathbf{y} is eliminated by a simple transformation, i. e.,

$$\begin{aligned} \mathbf{A}_k &= \bar{\mathbf{A}}_k - \bar{\mathbf{B}}_k \mathbf{D}_{22} (\mathbf{I} + \bar{\mathbf{D}}_k \mathbf{D}_{22})^{-1} \bar{\mathbf{C}}_k & ; & \quad \mathbf{B}_k = \bar{\mathbf{B}}_k - \bar{\mathbf{B}}_k \mathbf{D}_{22} (\mathbf{I} + \bar{\mathbf{D}}_k \mathbf{D}_{22})^{-1} \bar{\mathbf{D}}_k \\ \mathbf{C}_k &= (\mathbf{I} + \bar{\mathbf{D}}_k \mathbf{D}_{22})^{-1} \bar{\mathbf{C}}_k & ; & \quad \mathbf{D}_k = (\mathbf{I} + \bar{\mathbf{D}}_k \mathbf{D}_{22})^{-1} \bar{\mathbf{D}}_k \end{aligned} \quad (23)$$

Robustness Requirements in Robust Control

For the completeness of the derivation of robustness requirements, the physical system considered in this section is restricted to the so-called matched system, i.e., the system excited by the control effort (command) \mathbf{U} and disturbance \mathbf{d} (earthquakes or wind loads) through the same mechanism. The block diagram of such a physical system with active control is shown in Fig. 2 by the solid borders and lines. For the unmatched systems to which most structural systems belong, these robustness requirements derived can be still applied except that the performance will degrade to some degrees, depending on its situation.

In Fig. 2, the block \mathbf{P} is the structural system (plant system); the block \mathbf{K} is the controller system; \mathbf{r} is the reference signal for the tracking problem, \mathbf{U} is the control command generated from the controller; \mathbf{d} is the external disturbance such as the earthquake or wind loading, \mathbf{n} is the measurement noise and \mathbf{y} is the measured structural response; \mathbf{e} is the error signal which is the subtraction between the measured response and the reference. In the vibration suppression problems, the reference \mathbf{r} can be considered as a zero

signal and the same block diagram applies. It can be easily shown that the following relations in the frequency domain can be derived from the block diagram in Fig. 2;

$$\mathbf{y} = \mathbf{T}_0(\mathbf{r} - \mathbf{n}) + \mathbf{S}_0 \mathbf{P} \mathbf{d} \quad (24)$$

$$\mathbf{e} = \mathbf{S}_0 \mathbf{r} + \mathbf{T}_0 \mathbf{n} - \mathbf{S}_0 \mathbf{P} \mathbf{d} \quad (25)$$

in which \mathbf{S}_0 is the so-called sensitivity function and \mathbf{T}_0 is the complimentary sensitivity function, defined by

$$\mathbf{S}_0 = (\mathbf{I} + \mathbf{PK})^{-1} \quad ; \quad \mathbf{T}_0 = (\mathbf{I} + \mathbf{PK})^{-1} \mathbf{PK} \quad (26)$$

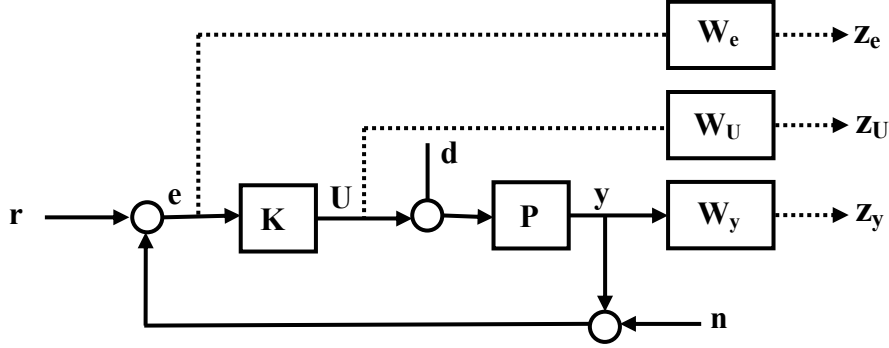


Fig. 2: Block Diagram of A Physical System with Active Control

The robustness requirements considered in active control should contain the performance robustness and stability robustness. As such, the performance robustness can include the resistance of influence from the reference \mathbf{r} , disturbance \mathbf{r} and measurement noise \mathbf{n} on the response \mathbf{y} or the error \mathbf{e} . Physically, the “size” of influence at any frequency can be quantitatively measured by the maximum value of the L_2 norm of the output vector (frequency domain) versus that of the corresponding input vector (frequency domain), which is mathematically bounded by the maximum singular value of the transfer function of the output versus input, denoted by $\bar{\sigma}(\cdot)$. Therefore, the performance robustness for the disturbance attenuation, tracking error and noise rejection in robust control can be described as follows [Zhou and Doyle (1998)]:

- (1) Disturbance Attenuation: for $\forall \omega \in R$, $\bar{\sigma}(\mathbf{H}_{yd}(\omega)) \ll 1$, i. e., $\bar{\sigma}(\mathbf{S}_0 \mathbf{P}) \ll 1$. Or more conservatively, we require $\bar{\sigma}(\mathbf{S}_0) \ll 1$.
- (2) Tracking Error: for $\forall \omega \in R$, $\bar{\sigma}(\mathbf{H}_{er}(\omega)) \ll 1$, i. e., $\bar{\sigma}(\mathbf{S}_0) \ll 1$.
- (3) Noise Rejection: for $\forall \omega \in R$, $\bar{\sigma}(\mathbf{H}_{yn}(\omega)) \ll 1$, i. e., $\bar{\sigma}(\mathbf{T}_0) \ll 1$.

From the relation $\mathbf{S}_0 + \mathbf{T}_0 = \mathbf{I}$, it is not possible to simultaneously achieve $\bar{\sigma}(\mathbf{S}_0) \ll 1$ and $\bar{\sigma}(\mathbf{T}_0) \ll 1$ for $\forall \omega \in R$. Fortunately, since the dominant frequency distribution of the disturbance \mathbf{d} (or reference \mathbf{r}) lies in the lower range and that of the noise \mathbf{n} lies in the higher range (as illustrated in Fig. 3), a possible trade-off between \mathbf{S}_0 and \mathbf{T}_0 can be achieved by specifying appropriate weighting functions \mathbf{W}_e and \mathbf{W}_y , which can be interpreted as the frequency distribution of \mathbf{d} (or \mathbf{r}) and \mathbf{n} , respectively, such that $\bar{\sigma}(\mathbf{W}_e \mathbf{S}_0) < 1$ and $\bar{\sigma}(\mathbf{W}_y \mathbf{T}_0) < 1$ for $\forall \omega \in R$. In other words, the performance robustness for the disturbance attenuation, tracking error and noise rejection can be expressed as

$$\|\mathbf{W}_e \mathbf{S}_0\|_{\infty} < 1 \quad (27)$$

$$\|\mathbf{W}_y \mathbf{T}_0\|_{\infty} < 1 \quad (28)$$

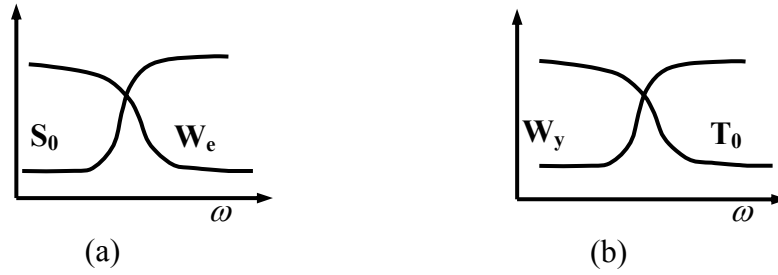


Fig. 3: (a) Frequency Distribution of S_0 and W_e ;
 (b) Frequency Distribution of T_0 and W_y

Another concerned issue in robustness requirements is the stability robustness, which is the retainability of stability with respect to system uncertainty. As in many literatures, system uncertainties are mostly classified into multiplicative and additive uncertainties for convenience of discussion. Their effects on the system stability and the corresponding conditions for stability robustness are described in the following [Zhou and Doyle (1998)]:

Additive Uncertainty

A plant system with additive uncertainty can be denoted by the set $\Pi = \{P + W_U \Delta : \Delta \text{ is a stable transfer function of uncertainty}\}$, in which W_U is a weighting matrix for modulating the “size” of Δ . For convenience of discussion, it can be properly adjusted to cover the bounds of all additive uncertainties in the frequency range considered such that $\|\Delta\|_\infty \leq 1$. The representation of the additive uncertainty in the block diagram of a physical system is shown in Fig. 4. By means of the linear fractional transformation (LFT), the block diagram in Fig. 4 can be converted into a simplified block diagram with an upper block Δ and a lower block $-W_U K S_0$, as shown in Fig. 5. The derivation is as follows. From Fig. 4, we observe $U = Ke = -Ky = -K(PU + o)$, therefore $U = -(I + KP)^{-1} K o$. Thus, $i = -W_U (I + KP)^{-1} K o = -W_U K (I + PK)^{-1} o = -W_U K S_0 o$. Furthermore, by the small gain theorem [Zhou and Doyle (1998)], it is obvious to reach that the system stability is guaranteed if

$$\|W_U K S_0\|_\infty < 1. \tag{29}$$

Therefore, Eq. (29) is a condition for the stability robustness.

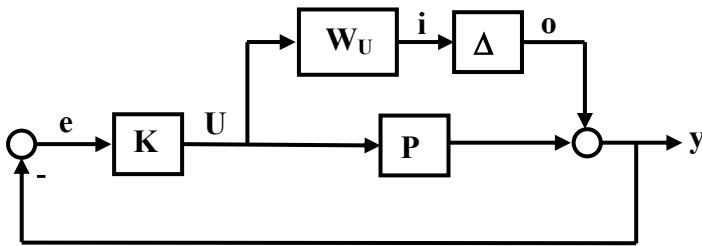


Fig. 4: Block Diagram with Additive Uncertainty

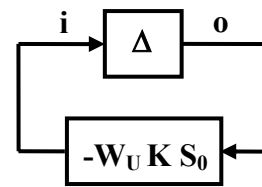


Fig. 5: Simplified Block Diagram with Additive Uncertainty after LFT

Multiplicative Uncertainty:

The plant system with the multiplicative uncertainty can be denoted by the set $\Pi = \{(I + W_y \Delta) P : \Delta \text{ is a stable transfer function of uncertainty}\}$, in which W_y is a weighting matrix for

modulating the “size” of Δ . For convenience of discussion, it is properly adjusted to cover the bounds of all multiplicative uncertainties in the frequency range considered such that $\|\Delta\|_\infty \leq 1$. The multiplicative uncertainty in the block diagram of a physical system is shown in Fig. 6. By means of the technique of linear fractional transformation, the block diagram in Fig. 6 can be converted into a simplified block diagram with an upper block Δ and a lower block $-\mathbf{W}_y \mathbf{T}_0$, as shown in Fig. 7. By the small gain theorem, it is concluded that the system stability is guaranteed if $\|\mathbf{W}_y \mathbf{T}_0\|_\infty < 1$, which is actually the same condition as Eq. (28).

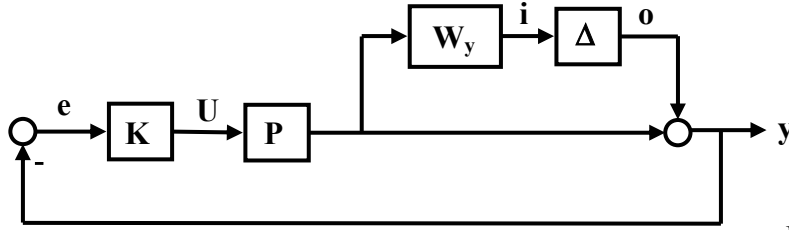


Fig. 6: Block Diagram with Multiplicative Uncertainty

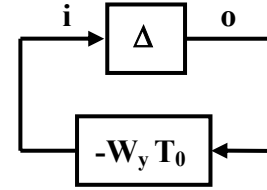


Fig. 7: Simplified Block Diagram with Additive Uncertainty after LFT

In summary, the robustness requirements for active control should at least contain the conditions of performance robustness and stability robustness, expressed in Eqs. (27)-(29). Conceptually, the transfer functions involved in these three conditions can be considered as the transfer functions from the reference \mathbf{r} to \mathbf{e} , \mathbf{U} and \mathbf{y} , multiplied by three weighting (filter) functions \mathbf{W}_e , \mathbf{W}_U and \mathbf{W}_y , respectively. Hence, the controlled outputs considered become three filtered quantities \mathbf{z}_e , \mathbf{z}_U and \mathbf{z}_y as denoted by the dotted line in Fig. 2.

The remaining task is to convert these three conditions into a generalized H_∞ problem presented in the next section.

Formulation of Robust H_∞ Control for Civil Structures

Let consider a civil structure subject to excitations with active control. Although the plant system of a civil structure is usually not a matched system, the block diagram presented in Fig. 2 with the reference signal $\mathbf{r} = 0$ is still used to help constructing the robust H_∞ controller. The price it pays is the degradation of the performance to some extent. Thus, the state equations of the plant system \mathbf{P} (civil structure), weightings \mathbf{W}_e , \mathbf{W}_U and \mathbf{W}_y are expressed by

$$\dot{\mathbf{X}}_P = \mathbf{A}_P \mathbf{X}_P + \mathbf{B}_P \mathbf{d} + \mathbf{E}_P \mathbf{U} \quad ; \quad \mathbf{y} = \mathbf{C}_P \mathbf{X}_P + \mathbf{D}_P \mathbf{d} + \mathbf{F}_P \mathbf{U} \quad (30)$$

$$\dot{\mathbf{X}}_e = \mathbf{A}_e \mathbf{X}_e + \mathbf{B}_e \mathbf{e} \quad ; \quad \mathbf{z}_e = \mathbf{C}_e \mathbf{X}_e + \mathbf{D}_e \mathbf{e} \quad (31)$$

$$\dot{\mathbf{X}}_U = \mathbf{A}_U \mathbf{X}_U + \mathbf{B}_U \mathbf{U} \quad ; \quad \mathbf{z}_U = \mathbf{C}_U \mathbf{X}_U + \mathbf{D}_U \mathbf{U} \quad (32)$$

and

$$\dot{\mathbf{X}}_y = \mathbf{A}_y \mathbf{X}_y + \mathbf{B}_y \mathbf{y} \quad ; \quad \mathbf{z}_y = \mathbf{C}_y \mathbf{X}_y + \mathbf{D}_y \mathbf{y} \quad (33)$$

, respectively, in which \mathbf{X}_P , \mathbf{X}_e , \mathbf{X}_U , \mathbf{X}_y are the state vectors; \mathbf{A}_P , \mathbf{B}_P , \mathbf{C}_P , \mathbf{D}_P , \mathbf{E}_P , \mathbf{F}_P , \mathbf{A}_e , \mathbf{B}_e , \mathbf{C}_e , \mathbf{D}_e , \mathbf{A}_U , \mathbf{B}_U , \mathbf{C}_U , \mathbf{D}_U , \mathbf{A}_y , \mathbf{B}_y , \mathbf{C}_y and \mathbf{D}_y are constant matrices in the state equations with appropriate dimensions. To account for the performance requirements expressed in Eqs. (27)-(29), the transfer functions from \mathbf{r} to \mathbf{z}_e , \mathbf{z}_U and \mathbf{z}_y are to be constructed. Besides, for the vibration suppression problem, it is esteemed necessary to also include the transfer functions from the external disturbance \mathbf{d} to \mathbf{z}_e , \mathbf{z}_U and \mathbf{z}_y for attenuation purpose. Thus, by considering \mathbf{r} and \mathbf{d} as the exogenous input, \mathbf{z}_e , \mathbf{z}_U and \mathbf{z}_y as

the controlled output \mathbf{z} , and \mathbf{e} as the measured output (because $\mathbf{e} = -\mathbf{y}$), the overall system to be controlled can be re-expressed as a generalized state equations written by

$$\begin{aligned}\dot{\mathbf{X}} &= \mathbf{A}\mathbf{X} + \mathbf{B}_1\mathbf{W} + \mathbf{B}_2\mathbf{U} \\ \mathbf{z} &= \mathbf{C}_1\mathbf{X} + \mathbf{D}_{11}\mathbf{W} + \mathbf{D}_{12}\mathbf{U} \\ \mathbf{e} &= \mathbf{C}_2\mathbf{X} + \mathbf{D}_{21}\mathbf{W} + \mathbf{D}_{22}\mathbf{U}\end{aligned}\quad (34)$$

in which

$$\begin{aligned}\mathbf{X} &= \begin{bmatrix} \mathbf{X}_P \\ \mathbf{X}_e \\ \mathbf{X}_U \\ \mathbf{X}_y \end{bmatrix}; \quad \mathbf{w} = \begin{bmatrix} \mathbf{r} \\ \mathbf{d} \end{bmatrix}; \quad \mathbf{z} = \begin{bmatrix} \mathbf{z}_e \\ \mathbf{z}_U \\ \mathbf{z}_y \end{bmatrix}; \quad \mathbf{A} = \begin{bmatrix} \mathbf{A}_P & 0 & 0 & 0 \\ -\mathbf{B}_e\mathbf{C}_P & \mathbf{A}_e & 0 & 0 \\ 0 & 0 & \mathbf{A}_U & 0 \\ \mathbf{B}_y\mathbf{C}_P & 0 & 0 & \mathbf{A}_y \end{bmatrix}; \quad \mathbf{B}_1 = \begin{bmatrix} 0 & \mathbf{B}_P \\ \mathbf{B}_e & -\mathbf{B}_e\mathbf{D}_P \\ 0 & 0 \\ 0 & \mathbf{B}_y\mathbf{D}_P \end{bmatrix}; \\ \mathbf{B}_2 &= \begin{bmatrix} \mathbf{E}_P \\ -\mathbf{B}_e\mathbf{F}_P \\ \mathbf{B}_U \\ \mathbf{B}_y\mathbf{F}_P \end{bmatrix}; \quad \mathbf{C}_1 = \begin{bmatrix} -\mathbf{D}_e\mathbf{C}_P & \mathbf{C}_e & 0 & 0 \\ 0 & 0 & \mathbf{C}_U & 0 \\ \mathbf{D}_y\mathbf{C}_P & 0 & 0 & \mathbf{C}_y \end{bmatrix}; \quad \mathbf{D}_{11} = \begin{bmatrix} \mathbf{D}_e & -\mathbf{D}_e\mathbf{D}_P \\ 0 & 0 \\ 0 & \mathbf{D}_y\mathbf{D}_P \end{bmatrix}; \quad \mathbf{D}_{12} = \begin{bmatrix} -\mathbf{D}_e\mathbf{F}_P \\ \mathbf{D}_U \\ \mathbf{D}_y\mathbf{F}_P \end{bmatrix} \\ \mathbf{C}_2 &= [-\mathbf{C}_P \quad 0 \quad 0 \quad 0]; \quad \mathbf{D}_{21} = [\mathbf{I} \quad -\mathbf{D}_P]; \quad \mathbf{D}_{22} = -\mathbf{F}_P\end{aligned}\quad (35)$$

The comparison of Eq. (34) and Eqs. (3)-(5) shows their similarity except that \mathbf{y} in Eq. (5) is replaced by \mathbf{e} for feedback. Thus, the LMI-based solution procedure mentioned in the earlier section can be used to design the robust H_∞ controller.

NUMERICAL SIMULATION

To demonstrate the applicability of the robust H_∞ controller presented to civil structures, extensive numerical simulations using the structural dynamics of a 3-story full-scale seismic-excited building are conducted. The building has a rectangular shape with a floor area of 4.5 m by 3m in each floor and a total height of 9 m (3m for each story), which was once constructed on the shake table of National Center for Research on Earthquake Engineering (NCREE) for experimental verification, as shown in Fig. 8. The masses of the building from the bottom to top floors are 1144.16, 1144.16 and 1113.62 kgf·s²/m, respectively. An active bracing system is connected between the ground and the first floor to provide the active force to the building for aseismic protection. Two earthquakes, the 1940 El Centro (100 seconds) and 1995 Kobe (60 seconds) earthquakes with a 0.1g PGA are used as the excitation sources. This actively controlled building has once been tested using LQG control and the results were presented in [Wu (2000)]. In [Wu (2000)], the numerical model of this actively controlled building was successfully constructed and the experimental verification has been done to shown its correctness. Therefore, this numerical model will be directly used as the true model system in the numerical simulation herein. The system matrices of this numerical model used can be found in the web site URL http://www.ce.tku.edu.tw/~jcwu/research/ncree_analytical.html. In this true system, the available responses of the building include the relative displacements x_i ($i = 1, 2, 3$) of each floor w.r.t. the ground, the absolute accelerations \ddot{x}_{ia} ($i = 1, 2, 3$) of each floor and the stroke x_f of actuator. The building with zero control command has three natural frequencies and damping ratios equal to 7.363, 22.933 and 37.966 rad/sec, and 1.38%, 2.46% and 1.32 %, respectively. For the comparison later, the response quantities of the building with zero command under earthquakes are tabulated in Table 1, and it is referred to as the “No Control” case in what follows. In Table 1, “Peak” represents the peak value in the whole time history, while “R.M.S.” represents the root-mean-square values within the dominant period from 24 s to 64 s for the El Centro earthquake and 14s to 54 s for the Kobe earthquake.



Fig. 8: 3-Story Full-Scale Building on the Shake Table of NCREE

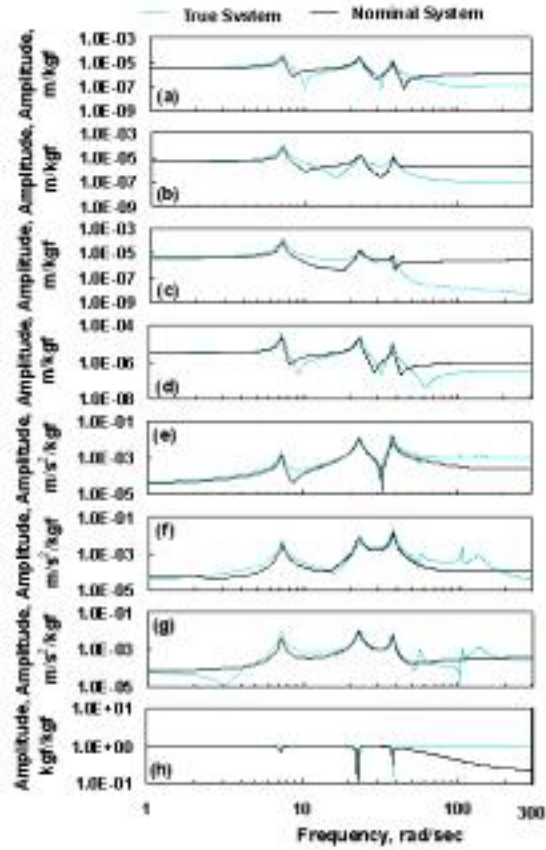


Fig. 9: Comparison of Transfer Functions of Response Quantities due to Actuator Command U ; (a) x_1 , (b) x_2 , (c) x_3 , (d) x_f , (e) \ddot{x}_{1a} , (f) \ddot{x}_{2a} , (g) \ddot{x}_{3a} , and (h) f .

Since the displacement and velocity measurements are not quite practical for implementation, the absolute accelerations of all three floors are used as the feedback quantities, i. e., $\mathbf{y} = [\ddot{x}_{1a}, \ddot{x}_{2a}, \ddot{x}_{3a}]^T$. However, all seven response quantities mentioned above will be computed. It should be noted that the 8-state nominal system used in [Wu (2000)] for LQG control is constructed through the balanced-state reduction method [Moore (1981)] from another system model which is identified with less accuracy than the true system. The transfer functions of the response quantities due to the actuator command U for the nominal system and the true system are plotted in Fig. 9 to illustrate the difference. It is observed from Fig. 9 that the size of the uncertainty is more significant than that just induced from the system reduction. This nominal system is also used in this paper for the robust H_∞ controller design in order to examine the robustness of the controller and make comparisons with the LQG results. Herein, the difference between the nominal system and the true system will be considered as the additive uncertainty and the weighting \mathbf{W}_U to be chosen should cover the bounds of all additive uncertainties.

Table 1: Response Quantities of the Actively Controlled Building with Zero Command (No Control)

(1)	El Centro (PGA=0.1g)		Kobe(PGA=0.1g)	
	Peak (2)	R.M.S (3)	Peak (4)	R.M.S (5)
x_1 (cm)	2.050	0.823	2.065	0.664
x_2 (cm)	4.592	1.766	4.493	1.428
x_3 (cm)	6.232	2.335	5.981	1.889
\ddot{x}_{1a} (g)	0.171	0.051	0.216	0.040
\ddot{x}_{2a} (g)	0.262	0.097	0.264	0.078
\ddot{x}_{3a} (g)	0.371	0.127	0.375	0.103

In this study, two robust H_∞ controllers are designed, denoted as $H_{\infty 1}$ and $H_{\infty 2}$, respectively. The design parameters for both controllers are chosen such that $H_{\infty 1}$ requires smaller control effort while $H_{\infty 2}$ requires bigger control effort, and the simulation results of them are compared with those of LQG₁ and LQG₂ controllers, which use the same measurements $y = [\ddot{x}_{1a}, \ddot{x}_{2a}, \ddot{x}_{3a}]^T$ for feedback, in [Wu (2000)], respectively. The weighting functions and other parameters used in the LMI computation for each controller are listed as follows: $\mathbf{W}_U = (4.4s + 200)/(11s + 440)$, $\mathbf{W}_e = (0.02s + 21000)/(0.5s + 10)$, $\mathbf{W}_y = (180s + 200)/(1.5s + 750)$, $\alpha=0.1589$, $\beta=0.1589$ and $\gamma_{\min}=200$ for the $H_{\infty 1}$ controller; $\mathbf{W}_U = (3.6s + 140)/(11s + 440)$, $\mathbf{W}_e = (0.02s + 28000)/(0.5s + 10)$, $\mathbf{W}_y = (180s + 200)/(1.5s + 750)$, $\alpha=0.1589$, $\beta=0.1589$ and $\gamma_{\min}=200$ for the $H_{\infty 2}$ controller. From the LMI-based solution procedure, the resultant attenuation value γ is equal to 4134.9 and 3161.1 for the $H_{\infty 1}$ and $H_{\infty 2}$ controller, respectively. Consequently, two 15-state ($k=15$) controllers are thus obtained, and they are further reduced to 8-state controller by the balanced-state reduction method [Moore (1981)] to facilitate implementation. The simulated responses under the two earthquakes of 0.1g PGA using the $H_{\infty 1}$ and $H_{\infty 2}$ controllers are tabulated in Columns (2)-(5) and Columns (11)-(14) of Table 2. In Table 2, the values inside the parentheses are the reduction percentages with respect to the ‘‘No Control’’ case in Table 1. As observed in Table 2, the reduction percentages of the RMS responses using the $H_{\infty 1}$ controller achieve about 50% with the control effort about 1000 kgf, while the reduction percentages of the RMS responses using $H_{\infty 2}$ are further improved toward 60% with the control effort about 1500 kgf. The reductions for the peak responses are relatively smaller and significant difference of reduction is observed for the two different earthquakes. For comparison, the simulated responses using LQG₁ and LQG₂ controllers [Wu (2000)] are also tabulated in Columns (6)-(9) and Columns (15)-(18) of Table 2, in which less effectiveness than H_∞ controllers is observed.

Table 2: Response Quantities of the Actively Controlled Building Using H^∞ Controllers

(1)	H^∞_1				LQG_1			
	El Centro (PGA=0.1g)		Kobe (PGA=0.1g)		El Centro (PGA=0.1g)		Kobe (PGA=0.1g)	
	Peak (2)	R.M.S (3)	Peak (4)	R.M.S (5)	Peak (6)	R.M.S (7)	Peak (8)	R.M.S (9)
x_1 (cm)	1.395 (32.0)	0.293 (64.4)	2.010 (2.7)	0.308 (53.7)	1.415 (31.0)	0.307 (62.7)	1.970 (4.6)	0.318 (52.1)
x_2 (cm)	2.475 (45.9)	0.589 (66.7)	3.962 (11.8)	0.606 (57.6)	2.736 (40.4)	0.651 (63.1)	4.051 (9.8)	0.656 (54.1)
x_3 (cm)	3.002 (51.8)	0.706 (69.8)	4.972 (16.9)	0.746 (60.5)	3.339 (46.4)	0.802 (65.7)	5.240 (12.4)	0.827 (56.2)
\ddot{x}_{1a} (g)	0.121 (29.0)	0.025 (50.5)	0.130 (40.0)	0.020 (48.5)	0.121 (29.0)	0.024 (52.9)	0.147 (31.9)	0.022 (45.0)
\ddot{x}_{2a} (g)	0.159 (39.5)	0.034 (65.0)	0.177 (32.8)	0.031 (60.7)	0.166 (36.6)	0.037 (61.9)	0.192 (27.3)	0.035 (55.1)
\ddot{x}_{3a} (g)	0.185 (50.2)	0.040 (68.7)	0.224 (40.3)	0.037 (64.2)	0.222 (40.2)	0.042 (66.9)	0.266 (29.1)	0.041 (60.2)
U (kgf)	1153	262	1782	275	1060	221	1424	224

(10)	H^∞_2				LQG_3			
	El Centro (PGA=0.1g)		Kobe (PGA=0.1g)		El Centro (PGA=0.1g)		Kobe (PGA=0.1g)	
	Peak (11)	R.M.S (12)	Peak (13)	R.M.S (14)	Peak (15)	R.M.S (16)	Peak (17)	R.M.S (18)
x_1 (cm)	1.289 (37.1)	0.255 (69.0)	1.813 (12.2)	0.274 (58.8)	1.339 (34.7)	0.261 (68.3)	1.924 (6.8)	0.288 (56.6)
x_2 (cm)	2.104 (54.2)	0.468 (73.5)	3.373 (24.9)	0.492 (65.6)	2.239 (51.2)	0.502 (71.6)	3.683 (18.0)	0.538 (62.3)
x_3 (cm)	2.270 (63.6)	0.544 (76.7)	4.062 (32.1)	0.589 (68.9)	2.653 (57.4)	0.604 (74.1)	4.557 (23.8)	0.663 (64.9)
\ddot{x}_{1a} (g)	0.104 (39.3)	0.023 (55.8)	0.117 (46.1)	0.018 (54.6)	0.101 (40.9)	0.020 (60.8)	0.128 (40.7)	0.020 (50.0)
\ddot{x}_{2a} (g)	0.149 (43.3)	0.029 (70.1)	0.135 (48.9)	0.024 (69.0)	0.133 (49.2)	0.027 (72.2)	0.157 (40.5)	0.026 (66.7)
\ddot{x}_{3a} (g)	0.149 (59.9)	0.032 (75.2)	0.155 (58.7)	0.028 (73.2)	0.170 (54.2)	0.033 (74.0)	0.198 (47.2)	0.033 (68.0)
U (kgf)	1706	365	2632	390	1657	323	2430	351

CONCLUDING REMARKS

The LMI-based H^∞ controller that takes into account the consideration of robust requirements that include the performance robustness on reducing the tracking error and in resistance to the external disturbance and measurement noise, and the stability robustness with respect to system uncertainty, has been introduced. The numerical model of the experimental full-scale 3-story seismic-excited building with a active bracing system, which has been verified through experiments in a literature, was used in the

simulation to verify its applicability toward actual implementation. In the extensive simulations, two earthquakes, the 1940 El Centro and 1995 Kobe earthquakes, are used as the excitations to the building. The system uncertainty is assumed in the controller design and acceleration measurements are used as the feedback quantities for practical consideration. Two H_∞ controllers are designed to successfully demonstrate the flexibility of modulating control effort in the approach. Furthermore, the simulation results of both H_∞ controllers are also compared with those of LQG controllers for their effectiveness. The simulation results have demonstrated that: (1) the LMI approach is efficient in computing the H_∞ controller; (2) the effectiveness of the H_∞ controllers presented is remarkable and its robustness with respect to disturbance attenuation, tracking error, noise rejection and uncertainty is satisfactory; (3) the performances of H_∞ controllers are slightly better than those of LQG controllers. Therefore, the LMI-based robust H_∞ control is suitable for the application to civil engineering buildings for aseismic protection.

REFERENCES

1. Basar, T and Bernhard, P (1991), H_∞ -Optimal Control and Related Min-max Design Problems- A Dynamic Game Approach, Birkhauser, Boston.
2. Casciati, F (editor) (2002), *Proceedings of Third World Conference on Structural Control*, John Wiley & Sons, N. Y.
3. Chung, L. L., Lin, R. C., Soong, T. T. and Reinhorn, A. M. (1989), "Experiments on Active Control for MDOF Seismic Structures", *ASCE Journal of Engineering Mechanics*, Vol. 115, No. 8, pp. 1609-1627.
4. Doyle, J. C., Glover, K., Khargonekar, P and Francis, B. (1989), "State Space Solutions to Standard H_2 and H_∞ Control Problems, *IEEE Transactions on Automatic Control*, Vol. 34, pp. 831-847.
5. Dyke, S. J., Spencer, B. F., Belknap, A. E., Ferrell, K. J., Quast, P. and Sain, M. K.(1994a), "Absolute Acceleration Feedback Control Strategies for the Active Mass Driver", *Proceedings of 1st World Conference on Structural Control*, Vol. 2, pp. TP1-51~TP1-60.
6. Dyke, S. J., Spencer, B. F., Quast, P., Sain, M. K., Kaspari, D. C. and Soong, T. T. (1994b), "Experimental Verification of Acceleration Feedback Control Strategies for an Active Tendon System", *National Center for Earthquake Engineering Research Technical Report*, NCEER-94-0024.
7. Gahinet, P. and Apkarian, P (1994), "A Linear Matrix Inequality Approach to H_∞ Control", *International Journal of Robust and Nonlinear Control*, Vol. 4, pp. 421-448.
8. Glover, K and Doyle, J. C. (1988), "State space Formula for All Stabilizing Controllers that Satisfy an H_∞ -norm Bound and Relations to Risk Sensitivity", *System and Control Letters*, Vol.11 pp. 167-172.
9. Kobori, T., Inoue, Y., Seto, K., Iemura, H. and Nishitani, A. (editors) (1998), *Proceedings of Second World Conference on Structural Control*, John Wiley & Sons, N. Y.
10. Moore, B. C. (1981), "Principal Component Analysis in Linear System: Controllability, Observability and Model Reduction", *IEEE Transactions on Automatic Control*, Vol. 26, No. 1, pp. 17-32.
11. Packard, A., Zhou, K., Pandey, P. and Becker, G. (1991), "A Collection of Robust Control Problems Leading to LMI", *Proceedings of the 30th Conference on Decision Control*, Brighton, England.
12. Soong, T. T., *Active Structural Control: Theory and Practice*, Longman Scientific & Technical.
13. Wu, J. C. (2000), "Modeling of an Actively Braced Full-Scale Building considering Control-Structure Interaction", *Earthquake Engineering and Structural Dynamics*, Vol. 29, pp. 1325-1342.
14. Wu, J. C. and Pan, B. C. (2002), "Wind Tunnel Verification of Actively Controlled High-Rise Building in Along-Wind Motion", *Journal of Wind Engineering and Industrial Aerodynamics*, Vol. 90, No.12-15, pp. 1933-1950.

15. Wu, J. C. and Cheng, L. Y. (2003), "Attack Angle Effects on Performance of Actively Controlled High-Rise Building Motion", Submitted for Possible Publication in *Journal of Wind Engineering and Industrial Aerodynamics*.
16. Zhou, K and Doyle, J. C. (1998), *Essentials of Robust Control*, Prentice Hall.

APPENDIX

Derivation of Eqs. (15) and (16) (excerpted from [Gahinet and Apkarian (1994)])

Projection lemma: For a symmetric matrix Ψ and two matrices \mathbf{P} and \mathbf{Q} , there exists a matrix $\boldsymbol{\theta}$ satisfying $\Psi + \mathbf{P}^T \boldsymbol{\theta}^T \mathbf{Q} + \mathbf{Q}^T \boldsymbol{\theta} \mathbf{P} < 0$ if and only if $\mathbf{W}_P^T \Psi \mathbf{W}_P < 0$ and $\mathbf{W}_Q^T \Psi \mathbf{W}_Q < 0$, in which \mathbf{W}_P and \mathbf{W}_Q are the matrices whose columns are composed of the null space bases of \mathbf{P} and \mathbf{Q} , respectively.

By the Projection lemma, the existence of a feasible $\boldsymbol{\theta}$ in Ineq. (12) requires the satisfaction of two conditions

$$\mathbf{W}_{\xi_{X_{cl}}}^T \Psi_{X_{cl}} \mathbf{W}_{\xi_{X_{cl}}} < 0 \quad (\text{A-1})$$

and

$$\mathbf{W}_{\psi}^T \Psi_{X_{cl}} \mathbf{W}_{\psi} < 0 \quad (\text{A-2})$$

, in which $\mathbf{W}_{\xi_{X_{cl}}}$ and \mathbf{W}_{ψ} are the matrices of null space bases of $\xi_{X_{cl}}$ and ψ , respectively. In Ineq. (A-1), \mathbf{X}_{cl} appears in $\Psi_{X_{cl}}$ and $\mathbf{W}_{\xi_{X_{cl}}}$ as well, therefore it needs further reduction as follows. From the observation that $\xi_{X_{cl}}$ can be expressed as

$$\xi_{X_{cl}} = \Phi \begin{bmatrix} \mathbf{X}_{cl} & 0 & 0 \\ 0 & \mathbf{I}_{m_1} & 0 \\ 0 & 0 & \mathbf{I}_{p_1} \end{bmatrix}; \quad \Phi = \left(\boldsymbol{\beta}^T, 0_{(k+m_2) \times m_1}, \zeta_{12}^T \right) \quad (\text{A-3})$$

, the null space matrices of $\xi_{X_{cl}}$ and Φ are related by the equation

$$\mathbf{W}_{\xi_{X_{cl}}} = \begin{bmatrix} \mathbf{X}_{cl}^{-1} & 0 & 0 \\ 0 & \mathbf{I}_{m_1} & 0 \\ 0 & 0 & \mathbf{I}_{p_1} \end{bmatrix} \mathbf{W}_{\Phi} \quad (\text{A-4})$$

The substitution of Eq. (A-4) into Ineq. (A-1) leads to

$$\mathbf{W}_{\Phi}^T \Phi_{X_{cl}} \mathbf{W}_{\Phi} < 0 \quad (\text{A-5})$$

in which

$$\Phi_{X_{cl}} = \begin{bmatrix} \mathbf{A}_0^T \mathbf{X}_{cl}^{-1} + \mathbf{X}_{cl}^{-1} \mathbf{A}_0^T & \mathbf{B}_0 & \mathbf{X}_{cl}^{-1} \mathbf{C}_0^T \\ \mathbf{B}_0^T & -\gamma \mathbf{I} & \mathbf{D}_{11}^T \\ \mathbf{C}_0 \mathbf{X}_{cl}^{-1} & \mathbf{D}_{11} & -\gamma \mathbf{I} \end{bmatrix} \quad (\text{A-6})$$

Now, we have obtained two Ineqs. (A-5) and (A-2) that guarantee the existence of a feasible \mathbf{X}_{cl} .

A further simplification of Ineq. (A-5) is performed by substituting the partition of \mathbf{X}_{cl} and \mathbf{X}_{cl}^{-1} expressed in Eq. (14) into $\Phi_{X_{cl}}$ in Eq. (A-6), i.e.,

$$\Phi_{X_{cl}} = \begin{bmatrix} \mathbf{AR} + \mathbf{RA}^T & \mathbf{AM} & \mathbf{B}_1 & \mathbf{RC}_1^T \\ \mathbf{M}^T \mathbf{A}^T & 0 & 0 & \mathbf{M}^T \mathbf{C}_1^T \\ \mathbf{B}_1^T & 0 & -\gamma \mathbf{I} & \mathbf{D}_{11}^T \\ \mathbf{C}_1 \mathbf{R} & \mathbf{C}_1 \mathbf{M} & \mathbf{D}_{11} & -\gamma \mathbf{I} \end{bmatrix} \quad (\text{A-7})$$

and expressing the null space matrix \mathbf{W}_Φ in Ineq. (A-5) as

$$\mathbf{W}_\Phi = \begin{bmatrix} \mathbf{W}_1 & 0 \\ 0 & 0 \\ 0 & \mathbf{I}_{m_1} \\ \mathbf{W}_2 & 0 \end{bmatrix} \quad (\text{A-8})$$

in which $\begin{bmatrix} \mathbf{W}_1 \\ \mathbf{W}_2 \end{bmatrix} = \mathbf{N}_R$ is the null space matrix of $[\mathbf{B}_2^T \quad \mathbf{D}_{12}^T]$. By this, Ineq. (A-5) is rewritten as

$$\begin{bmatrix} \mathbf{W}_1 & 0 \\ 0 & \mathbf{I}_{m_1} \\ \mathbf{W}_2 & 0 \end{bmatrix}^T \begin{bmatrix} \mathbf{AR} + \mathbf{RA}^T & \mathbf{B}_1 & \mathbf{RC}_1^T \\ \mathbf{B}_1^T & -\gamma \mathbf{I} & \mathbf{D}_{11}^T \\ \mathbf{C}_1 \mathbf{R} & \mathbf{D}_{11} & -\gamma \mathbf{I} \end{bmatrix} \begin{bmatrix} \mathbf{W}_1 & 0 \\ 0 & \mathbf{I}_{m_1} \\ \mathbf{W}_2 & 0 \end{bmatrix} < 0 \quad (\text{A-9})$$

or rearranged as

$$\begin{bmatrix} \mathbf{N}_R & 0 \\ 0 & \mathbf{I}_{m_1} \end{bmatrix}^T \begin{bmatrix} \mathbf{AR} + \mathbf{RA}^T & \mathbf{RC}_1^T & \mathbf{B}_1 \\ \mathbf{C}_1 \mathbf{R} & -\gamma \mathbf{I} & \mathbf{D}_{11} \\ \mathbf{B}_1^T & \mathbf{D}_{11}^T & -\gamma \mathbf{I} \end{bmatrix} \begin{bmatrix} \mathbf{N}_R & 0 \\ 0 & \mathbf{I}_{m_1} \end{bmatrix} < 0 \quad (\text{A-10})$$

In a similar manner, Ineq. (A-1) can be rewritten as

$$\begin{bmatrix} \mathbf{N}_S & 0 \\ 0 & \mathbf{I}_{p_1} \end{bmatrix}^T \begin{bmatrix} \mathbf{AS} + \mathbf{A}^T \mathbf{S} & \mathbf{SB}_1^T & \mathbf{C}_1^T \\ \mathbf{B}_1^T \mathbf{S} & -\gamma \mathbf{I} & \mathbf{D}_{11} \\ \mathbf{B}_1^T & \mathbf{D}_{11}^T & -\gamma \mathbf{I} \end{bmatrix} \begin{bmatrix} \mathbf{N}_R & 0 \\ 0 & \mathbf{I}_{p_1} \end{bmatrix} < 0 \quad (\text{A-11})$$